Spectroscopy of ^{123}Cs: Configuration dependent crossing frequencies

J. R. Hughes, D. B. Fossan, D. R. LaFosse, Y. Liang,* P. Vaska, M. P. Waring, and J.-Y. Zhang†

Department of Physics, State University of New York at Stony Brook, Stony Brook, New York 11794

(Received 5 December 1991)

Several collective structures have been populated in the $Z=55$ nucleus ^{123}Cs following the ^{108}Pd(^{19}F,4n) fusion-evaporation reaction at a beam energy of 76 MeV. The low-lying structure is found to be dominated by a decoupled rotational band built on the unique-parity $\pi h_{11/2}$ orbital. Rotational structures based on the normal-parity $g_{7/2}$ proton and the $g_{9/2}$ proton-hole orbitals are also observed. Rotational alignments occur in the $\pi h_{11/2}$ band at $\hbar\omega_c \approx 0.44$ MeV, and in the $\pi g_{9/2}^{-1}$ band at $\hbar\omega_c = 0.38$ MeV, both attributed to the rotational alignment of a pair of $h_{11/2}$ neutrons, despite the different crossing frequency. In addition, the γ-vibrational band built on the $\pi h_{11/2}$ orbital has been observed feeding both signatures of the corresponding rotational cascade. These results are compared to cranked shell model calculations and to the systematics of the region.

PACS number(s): 25.70.−z, 27.60.+j

I. INTRODUCTION

The neutron deficient nuclei in the $A \sim 120$ mass region have been of considerable interest in recent years. These nuclei lie in a transitional region where the number of valence nucleons outside the spherical $^{114}_{50}$Sn$_{64}$ core is sufficient to induce a quadrupole nuclear deformation which is generally soft [1,2] with respect to γ, the triaxiality parameter [3]. As such, both valence neutrons and protons are expected to have strong and specific shape driving forces on the core when occupying high-j orbitals that are close to the Fermi surface. For the neutron deficient cesium nuclei, the proton Fermi surface lies just below the $h_{11/2}$ subshell. The active proton orbitals are $g_{7/2}(d_{5/2})$, the $g_{9/2}$ extruder, and the unique-parity $h_{11/2}$ intruder. The neutron Fermi surface lies in the $h_{11/2}$ midshell.

Cranked shell model (CSM) calculations suggest that the first band crossing in this region is due to the rotational alignment of a pair of $h_{11/2}$ neutrons. The band structure above the first neutron crossing, that often identifies the configuration, is sensitive to the resulting nuclear shape (γ). The shape driving force of the aligned pair depends on the position of the neutron Fermi surface within the $h_{11/2}$ subshell; neutrons in the upper midshell favor a collective oblate shape, while those in the lower midshell favor collective prolate shapes.

Furthermore, the neutron crossing frequency is expected to be sensitive to the position of the neutron Fermi surface. CSM calculations suggest that the neutron crossing frequency should decrease as the neutron Fermi surface approaches the $\Omega = \frac{1}{2}$ component of the $h_{11/2}$ orbital. However, recent results in light ^{117,119}I [4,5] nuclei indicate that the $h_{11/2}$ neutron alignment is delayed in the $\pi h_{11/2}$ band relative to that in the $g_{9/2}$ proton-hole band. Similar effects have previously been reported in the $A \sim 160$–170 region [6], where it is suggested that an enhanced quadrupole deformation is responsible for the delayed crossing frequency.

Two structure features recently observed in light iodine isotopes indicate the stability of an oblate shape. One feature involves a collective oblate ($\gamma = -60°$) shape, while the other involves a noncollective oblate ($\gamma = +60°$) shape. Both of these features are possibly related to a $Z = 54$ oblate shell gap [7–9]. Collective oblate and prolate single-quasiparticle bands based on the $\pi h_{11/2}$ and $\pi g_{7/2}(d_{5/2})$ orbitals have been found to coexist in odd-mass $^{119-125}$I [8,5,10,11] isotopes. In addition, band terminating noncollective oblate structures have been found at moderate angular momentum in ^{121}I [12], an isotone of ^{123}Cs, as well as in ^{115,117,119}I [4,5]. The even-even ^{118,122}Xe [13,14] nuclei have also been found to display a termination of the rotational structure, whereas similar investigations in $Z = 56$ Ba nuclei have proved inconclusive [15]. None of these features have so far been observed in Cs isotopes.

The ^{123}Cs nucleus has been studied as part of a systematic investigation of the odd-Z Cs isotopes [10,16–18] to explore these interesting structure properties. Low-lying levels in ^{123}Cs have previously been reported by Beyer *et al.* [19], and Arlt *et al.* [20], following the β^+ decay of ^{123}Ba, and coincident γ rays by Garg, Sjoreen, and Fossan [21], and Hattula *et al.* [22] utilizing heavy-ion fusion-evaporation reactions. Preliminary results of this work have previously been presented [23].

II. EXPERIMENTAL METHODS AND RESULTS

Excited states in ^{123}Cs were populated with the ^{108}Pd(^{19}F,4n) fusion-evaporation reaction at a beam ener-

*Present address: Argonne National Laboratory, 9700 S. Cass Avenue, Argonne, IL 60439.

†Present address: University of Tennessee, Knoxville, TN 37996. (On leave from Institute of Modern Physics, Lanzhou, China.)

gy of 76 MeV. The ^{19}F beam was provided by the Stony Brook FN tandem accelerator. The target consisted of 2.5 mg/cm^2 of ^{108}Pd rolled onto a Pb backing of 50 mg/cm^2. The present series of experiments involved γ-ray excitation function, γ-γ coincidence, and γ-ray angular distribution measurements.

The γ-ray excitation functions and γ-γ coincidence data were obtained using an array of six n-type Ge detectors, each with a relative efficiency of 25% at $E_\gamma = 1.3$ MeV. Each Ge detector was operated in conjunction with a transverse bismuth germanate (BGO) suppression shield [24] to reduce the Compton background. A coincidence resolving time of $2\tau = 100$ ns was used to collect the γ-γ data.

In addition, multiplicity information was collected with fourteen closely packed hexagonal BGO detectors, seven above and seven below the target chamber. An energy threshold of 100 keV was set on each detector, well above the Pb x rays. A hardware trigger requirement of at least two BGO detectors and two Ge detectors was set in order to reduce the contribution from Coulomb excitation and radioactivity. With this condition, approximately 81 million events were collected. These data were subsequently sorted offline to produce a symmetrized $2k \times 2k$ matrix, which was used in the construction of the ^{123}Cs level scheme. Typical γ-γ coincidence spectra are shown in Fig. 1.

The γ-ray angular distribution measurements were performed at five angles with one of the Compton-suppressed Ge detectors (CSG), along with a fixed monitor detector. The empirical γ-ray intensities were fitted to the formula

$$W(\theta) = A_0 + A_2 P_2(\cos\theta) + A_4 P_4(\cos\theta)$$

where θ is the detector angle relative to the beam direction, P_n are Legendre polynomials, and A_n are adjustable parameters. The resulting A_n values provide multipolarity information on the γ-ray transitions. The deduced A_2/A_0 and A_4/A_0 values for a number of $E2$ transitions were used to extract the average empirical alignment parameters, $\alpha_2 = 0.71(10)$ and $\alpha_4 = 0.19(10)$, from a comparison with theoretical values [25]. Using these alignment parameters the multipole mixing ratio δ was extracted for a number of $\Delta J = 1$ transitions with a χ^2 minimization technique [26].

Table I presents extracted energies, relative intensities, angular distribution coefficients, mixing ratios, and spin-parity assignments for all the transitions assigned to ^{123}Cs. The intensities are obtained from a combination of singles and coincidence data.

The decay scheme of ^{123}Cs as deduced from the present series of experiments is shown in Fig. 2, where the ordering of the γ rays has been determined from coincidence relationships and relative intensities. The spin-parity assignments are based on the angular distribution results and the systematics of the neighboring odd-Z nuclei. The levels naturally form several bands, which have been labeled 1–4. Bands 2 and 3 have been assigned bandhead spin-parities $\frac{9}{2}^+$ and $\frac{11}{2}^-$, respectively, in accordance with the angular distributions of the 201-keV transition to the known $\frac{5}{2}^+$ state [19], and the pure dipole nature of the 137-keV transition. These assignments are in agreement with those previously made by Garg *et al.* [21] and Arlt *et al.* [20]. Band 1 has been assigned a tentative bandhead spin-parity $(\frac{7}{2}^+)$ based on the systematics of the neighboring odd-Z nuclei. Coincidence relationships determine that the $(\frac{7}{2}^+)$ state lies higher in energy than

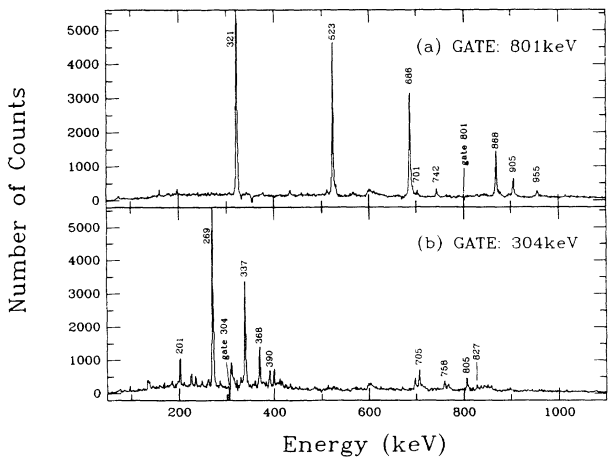

FIG. 1. Typical γ-γ spectra gated on (a) the 801-keV transition in band 3, and (b) the 304-keV transition in band 2. Coincident γ rays are labeled with their energies in keV.

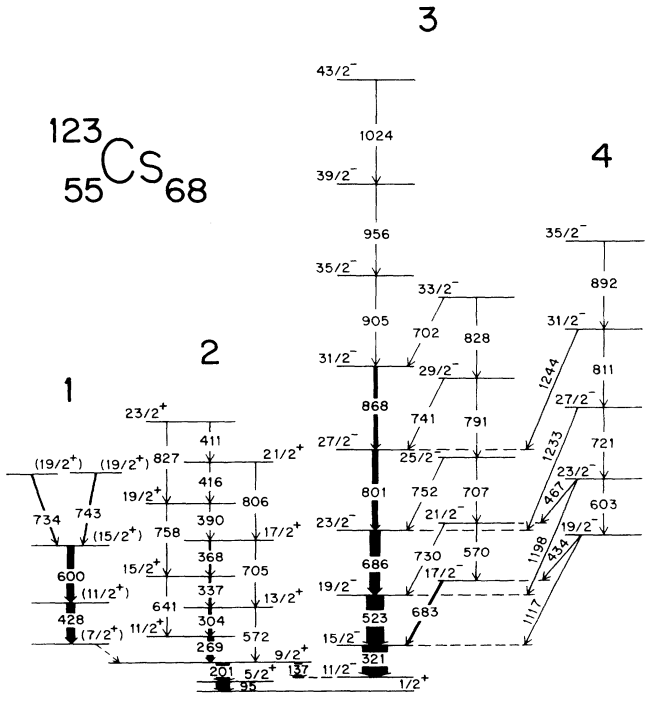

FIG. 2. The decay scheme for ^{123}Cs deduced from the present work. The transitions are labeled with their energies in keV, and the width of the arrows represents the relative intensities. Spin-parity assignments are tentative for all but the low-lying states, as described in the text.

TABLE I. Energies, relative intensities, angular distributions, and spin-parity assignments for the transitions assigned to ^{123}Cs following the ^{108}Pd(^{19}F,4n) reaction at 76 MeV.

E_γ[a] (keV)	Relative[b] intensity	A_2/A_0	A_4/A_0	Multipolarity mixing ratio	$J_i^\pi \rightarrow J_f^\pi$
95.0	20(5)			($E2$)	$\frac{5}{2}^+ \rightarrow \frac{1}{2}^+$
136.7	27(2)	−0.09(8)	0.03(10)	$E1$	$\frac{9}{2}^+ \rightarrow \frac{11}{2}^-$
				$\delta = -0.04(10)$	
200.7	55(4)	0.184(57)	−0.038(70)	$E2$	$\frac{9}{2}^+ \rightarrow \frac{5}{2}^+$
269.0	25(1)	0.027(47)	0.030(97)	$M1/E2$	$\frac{11}{2}^+ \rightarrow \frac{9}{2}^+$
				$\delta = +0.17(2)$	
303.8	14(1)	−0.013(49)	0.039(63)	$M1/E2$	$\frac{13}{2}^+ \rightarrow \frac{11}{2}^+$
				$\delta = +0.14(4)$	
320.5	≡100	0.297(28)	−0.043(45)	$E2$	$\frac{15}{2}^- \rightarrow \frac{11}{2}^-$
336.9	9(1)	0.044(64)	0.052(81)	$M1/E2$	$\frac{15}{2}^+ \rightarrow \frac{13}{2}^+$
				$\delta = +0.18(5)$	
367.9	4(1)			$M1/E2$	$\frac{17}{2}^+ \rightarrow \frac{15}{2}^+$
389.5	2(1)			$M1/E2$	$\frac{19}{2}^+ \rightarrow \frac{17}{2}^+$
416.2	∼1			$M1/E2$	$\frac{21}{2}^+ \rightarrow \frac{19}{2}^+$
410.5	<1			$M1/E2$	$\frac{23}{2}^+ \rightarrow \frac{21}{2}^+$
428.3	34(3)			($E2$)	$\frac{13}{2}^+ \rightarrow \frac{9}{2}^+$
433.6	4(1)			($M1/E2$)	$\frac{19}{2}^- \rightarrow \frac{17}{2}^-$
466.6	∼1			($M1/E2$)	$\frac{23}{2}^- \rightarrow \frac{21}{2}^-$
522.6	68(3)	0.280(40)	−0.024(46)	$E2$	$\frac{19}{2}^- \rightarrow \frac{15}{2}^-$
570.0	2(1)			($E2$)	$\frac{21}{2}^- \rightarrow \frac{17}{2}^-$
572.4	<1			$E2$	$\frac{13}{2}^+ \rightarrow \frac{9}{2}^+$
600.3	30(3)			($E2$)	$\frac{17}{2}^+ \rightarrow \frac{13}{2}^+$
602.9	2(1)			($E2$)	$\frac{23}{2}^- \rightarrow \frac{19}{2}^-$
640.5	3(1)			$E2$	$\frac{15}{2}^+ \rightarrow \frac{11}{2}^+$
682.7	11(2)	−0.653(49)	0.006(67)	$M1/E2$	$\frac{17}{2}^- \rightarrow \frac{15}{2}^-$
				$\delta = -0.36(2)$	
685.5	43(1)	0.429(45)	0.033(51)	$E2$	$\frac{23}{2}^- \rightarrow \frac{19}{2}^-$
701.7	∼1			($M1/E2$)	$\frac{33}{2}^- \rightarrow \frac{31}{2}^-$
704.5	2(1)			$E2$	$\frac{17}{2}^+ \rightarrow \frac{13}{2}^+$
706.9	2(1)			($E2$)	$\frac{25}{2}^- \rightarrow \frac{21}{2}^-$
721.0	2(1)			($E2$)	$\frac{27}{2}^- \rightarrow \frac{23}{2}^-$
730.4	5(1)			($M1/E2$)	$\frac{21}{2}^- \rightarrow \frac{19}{2}^-$
734.2	5(2)			($E2$)	$(\frac{21}{2}^+) \rightarrow \frac{17}{2}^+$
741.4	∼1			($M1/E2$)	$\frac{29}{2}^- \rightarrow \frac{27}{2}^-$
743.2	6(2)			($E2$)	$(\frac{21}{2}^+) \rightarrow \frac{17}{2}^+$
751.5	3(1)			($M1/E2$)	$\frac{25}{2}^- \rightarrow \frac{23}{2}^-$
757.9	2(1)			$E2$	$\frac{19}{2}^+ \rightarrow \frac{15}{2}^+$
791.0	2(1)			($E2$)	$\frac{29}{2}^- \rightarrow \frac{25}{2}^-$
800.6	18(1)	0.355(51)	−0.043(58)	$E2$	$\frac{27}{2}^- \rightarrow \frac{23}{2}^-$
805.7	2(1)			$E2$	$\frac{21}{2}^+ \rightarrow \frac{17}{2}^+$
811.4	∼1			($E2$)	$\frac{31}{2}^- \rightarrow \frac{27}{2}^-$
826.7	∼1			$E2$	$\frac{23}{2}^+ \rightarrow \frac{19}{2}^+$
828.4	∼1			($E2$)	$\frac{33}{2}^- \rightarrow \frac{29}{2}^-$
868.3	8(1)	0.458(48)	−0.057(59)	$E2$	$\frac{31}{2}^- \rightarrow \frac{27}{2}^-$

TABLE I. (*Continued*).

E_γ[a] (keV)	Relative[b] intensity	A_2/A_0	A_4/A_0	Multipolarity mixing ratio	$J_i^\pi \rightarrow J_f^\pi$
891.8	<1			(*E*2)	$(\frac{35}{2}^-) \rightarrow \frac{31}{2}^-$
904.6	3(1)			(*E*2)	$\frac{35}{2}^- \rightarrow \frac{31}{2}^-$
955.5	~1			(*E*2)	$\frac{39}{2}^- \rightarrow \frac{35}{2}^-$
1024.0	<1			(*E*2)	$(\frac{43}{2}^-) \rightarrow \frac{39}{2}^-$
1116.6	~1			(*E*2)	$\frac{19}{2}^- \rightarrow \frac{15}{2}^-$
1197.7	~1			(*E*2)	$\frac{23}{2}^- \rightarrow \frac{19}{2}^-$
1233.3	~1			(*E*2)	$\frac{27}{2}^- \rightarrow \frac{23}{2}^-$
1243.8	~1			(*E*2)	$\frac{31}{2}^- \rightarrow \frac{27}{2}^-$

[a]Gamma-ray energies are accurate to within ±0.3 keV.
[b]Transition intensities are corrected for Ge efficiency, and are obtained from a combination of singles and coincidence data.

the 296-keV $\frac{9}{2}^+$ state; the linking transition is not observed in the present data possibly due to significant internal conversion arising from the $M1/E2$ character for a low transition energy. Band 4 has been assigned a bandhead spin and parity $\frac{19}{2}^-$ based on the nature of its depopulation to both signature components of band 3, and the systematics of this band structure in this region.

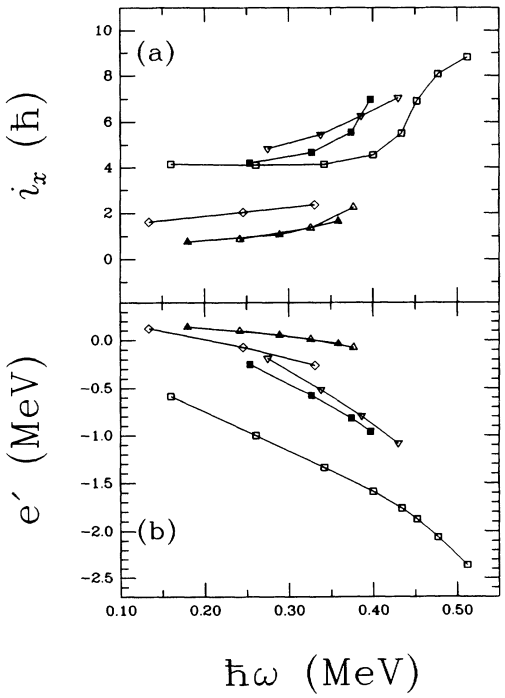

FIG. 3. (a) Experimental alignments, and (b) Routhians, for the positive-parity band 1 (diamonds), band 2 (triangles), the negative-parity band 3 (squares) and band 4 (inverted triangles). Solid (open) symbols are used for the signature component $\alpha=+\frac{1}{2}(-\frac{1}{2})$. A reference rotor ($\mathcal{I}_0=17.0\hbar^2$ MeV^{-1} and $\mathcal{I}_1=25.8\hbar^4$ MeV^{-3}) has been subtracted in each case.

III. DISCUSSION

In order to facilitate the discussion, the experimentally determined spins and level energies have been transformed into the rotating frame of reference following the prescription of Bengtsson and Frauendorf [27]. The Harris parameters [28], $\mathcal{I}_0=17.0\hbar^2$ MeV^{-1} and $\mathcal{I}_1=25.8\hbar^4$ MeV^{-3}, derived from a fit to the low-lying members of the $\pi h_{11/2}$ band, define a frequency dependent reference moment of inertia, which has been used to obtain the experimental alignments i_x and Routhians e' in the usual manner. The results of this procedure are displayed in Fig. 3, and the quasiparticle configurations assigned to the bands in ^{123}Cs are summarized in Table II.

A. Positive-parity configurations

Two positive-parity bands have been observed in ^{123}Cs by the present series of experiments. Band 1, built on the $(\frac{7}{2}^+)$ state, is associated with a $\pi g_{7/2}$ configuration at a prolate deformation of $\epsilon_2 \sim 0.2$. For this position of the proton Fermi surface, the $\pi g_{7/2}, \Omega=\frac{3}{2}$ orbital gives rise to a decoupled band, with only the $\alpha=-\frac{1}{2}$ signature component being observed. Similar bands have previously been observed in the ^{125,127}Cs isotopes [17,18].

Band 2 has been assigned a $g_{9/2}$ proton-hole configuration. The $\Omega=\frac{9}{2}$ component of the $\pi g_{9/2}$ orbital, which originates from below the $Z=50$ shell closure, becomes energetically favorable at a prolate deformation of

TABLE II. Assigned configurations for the bands in ^{123}Cs.

Band	(π,α)	Configuration	Label
1	$(+,-\frac{1}{2})$	$\pi g_{7/2}$	*G*
2	$(+,\pm\frac{1}{2})$	$\pi g_{9/2}^{-1}$	*E,F*
3	$(-,\pm\frac{1}{2})$	$\pi h_{11/2}$	*A,B*
	$(-,\pm\frac{1}{2})$	$\pi h_{11/2} \otimes [\nu h_{11/2}]^2$	*Aab,Bab*
4	$(-,-\frac{1}{2})$	$\pi h_{11/2} \otimes \gamma$ − vib	

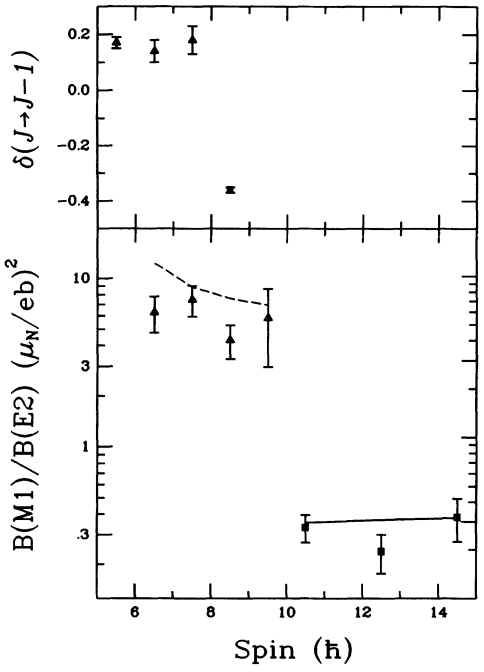

FIG. 4. Experimental $B(M1)/B(E2)$ ratios (bottom) and mixing ratios (top) for a number of transitions in band 2 (triangles), and band 3 (squares). The solid line is the result of a calculation for the $\pi h_{11/2}$ orbital using the semiclassical model of Dönau and Frauendorf [31], assuming $\gamma=-10°$ and $K=\frac{3}{2}$. The dashed line is for the $\pi g_{9/2}^{-1}$ orbital with $\gamma=0°$ and $K=\frac{9}{2}$.

$\epsilon_2\sim 0.26$. This high-Ω value is responsible for the strongly coupled nature (signature splitting $\Delta e'\sim 0$) of this band. In addition, the $\Delta J=1$ transitions linking states of opposite signature are relatively strong compared to the $E2$ crossover transitions [$B(M1)/B(E2)\sim 10(\mu_N/e\ \mathrm{b})^2$, see Fig. 4], resulting from the large positive g factor and the large K value of the $\pi g_{9/2}$ orbital. Similar band structures have systematically been observed throughout the light Sb, I, and Cs nuclei [21,29].

B. Negative-parity configurations

Band 3 is assigned the unique-parity $\pi h_{11/2}, \Omega=\frac{1}{2}$ configuration. The band consists of two $\Delta J=2$ cascades initiating on the $J^\pi=\frac{11}{2}^-$ and $\frac{17}{2}^-$ states corresponding to the signature components $\alpha=-\frac{1}{2}$ and $+\frac{1}{2}$, respectively. The signature splitting between the two cascades is large, as expected for a low-K band. $\Delta J=1$ transitions have been observed depopulating the unfavored to the favored signature, and the ratios of the reduced transition probabilities with respect to the inband $E2$ transitions have been measured. As was found in ^{125,127}Cs [17,18], and ^{131}La [30], the geometrical model of Dönau and Frauendorf [31] underestimates these ratios by up to an order of magnitude assuming prolate axial symmetry; agreement may be obtained, however, by introducing a degree of triaxiality [18,32]. TRS calculations [33] suggest that the two signatures of the $\pi h_{11/2}$ configuration are associated with different, but nonzero γ values. In addition, the signature splitting $\Delta e'$ in the $\pi h_{11/2}$ band decreases as a function of the rotational frequency $\hbar\omega$. CSM calculations indicate that the alignment of a pair of $h_{11/2}$ neutrons would induce a degree of triaxiality ($\gamma\sim -15°$) in the γ-soft core. The signature splitting of the $\pi h_{11/2}$ orbital is expected to decrease as γ decreases from 0°.

The two structure features related to oblate shapes in this mass region are of major interest in the Cs nuclei. The possibility of noncollective oblate terminating states, as observed in ^{121}I [12], has been examined in ^{123}Cs. A search for any irregularities in the rotational character of the $\pi h_{11/2}$ band has been made, but none were found up to the highest experimentally observed spin of ($\frac{43}{2}$). The most favored terminating state in ^{121}I is $J=\frac{39}{2}$ [12], and those in ^{118,122}Xe occur at $J\sim 30$ and $J=23$, respectively [13,14]. None, however, has been found in ^{121}Xe up to $J=\frac{39}{2}$ [34], or in ^{122,123,124}Ba up to spins of (30), $\frac{67}{2}$, and 32, respectively [15]. In addition, no collective oblate single-quasiparticle bands have been found in the present study of ^{123}Cs, or in similar studies of ^{125,127,129}Cs [17,18,35], despite the experimentally well documented characteristics of such bands observed in odd-even iodine isotopes [8,5,10,11].

The absence of these oblate structures in the Cs isotopes is possibly related to the single-particle level structure around the $Z=54$ oblate shell gap. For Cs isotopes ($Z=55$), all the levels below the $Z=54$ gap are occupied, and thus the proton pairing is expected to be reduced. In I isotopes, with the availability of unoccupied orbitals below the $Z=54$ gap, the proton pairing is expected to stabilize the oblate shape. The proton pairing energy difference in addition to the shell energy correction difference in Cs and I, perhaps explains the lack of oblate stability for the Cs $\pi h_{11/2}$ oblate configuration.

Band 4 is interpreted as a $\pi h_{11/2}$ quasiparticle band coupled to the γ vibration of the core. Each level within this structure is characterized by a strong $E2$ transition feeding the favored signature of the corresponding rotational band. Similar structures have been observed in odd-Z ^{119,121,125,127}Cs [10,16,17,18], and in the $N=68$ even-even isotones ^{122}Xe [22] and ^{124}Ba [36]. The spin-parity assignments are made on the basis of systematics and the observation of both $J\rightarrow J$ and $J\rightarrow J-2$ transitions de-exciting this band.

C. The $[\nu h_{11/2}]^2$ crossing

Band crossings are observed in both the $\pi g_{9/2}^{-1}$ and the $\pi h_{11/2}$ structures in ^{123}Cs. Band 3 is crossed at a rotational frequency $\hbar\omega\approx 0.44$ (0.41) MeV in the favored (unfavored) component, with a corresponding gain in alignment of $\Delta i_x\sim 5\hbar$. This crossing frequency has been obtained by extrapolating the alignments at low and high frequency to the crossing point (this procedure introduces a small uncertainty into the extracted value, which is indicated in Fig. 6). In accordance with the systematic identification of the $[\nu h_{11/2}]^2$ alignment (ab) in the

heavier Cs isotopes [10,17,18], the observed upbend in the yrast band of ^{123}Cs is attributed to the rotational alignment of a pair of $h_{11/2}$ neutrons. CSM results indicate that the alternative interpretation of a $[\pi h_{11/2}]^2$ alignment can be ruled out, as the *BC* alignment is predicted to occur at $\hbar\omega \sim 0.70$ MeV (the *AB* alignment is Pauli blocked in the $\pi h_{11/2}$ band). Band 2 shows an increase in alignment at a frequency $\hbar\omega \approx 0.38$ MeV. CSM calculations (see below) indicate that the $[\nu h_{11/2}]^2$ crossing should occur at a frequency of $\hbar\omega \approx 0.40$ MeV, whereas the $[\pi h_{11/2}]^2$ crossing should occur at $\hbar\omega \approx 0.42$ MeV. The alignment in band 2 is therefore interpreted as the onset of the $[\nu h_{11/2}]^2$ pair alignment, although the alternative $[\pi h_{11/2}]^2$ alignment cannot be ruled out. The alignment of band 2 is compared to that of the other $\pi g_{9/2}^{-1}$ bands in the odd-Cs isotopes in Fig. 5.

The experimentally observed *ab* neutron crossing frequencies in the $\pi h_{11/2}$ and $\pi g_{9/2}^{-1}$ bands in a number of odd-Cs isotopes are displayed in Fig. 6. This crossing is not observed in the $\pi g_{9/2}^{-1}$ bands of ^{125,127}Cs below the experimentally observed highest rotational frequencies $\hbar\omega \sim 0.45$ and 0.40 MeV, respectively. The *ab* crossing frequency shows a clear dependence on the configuration for the $N \leq 68$ isotopes. For the $\pi h_{11/2}$ bands, the crossing frequency remains fairly constant across the isotopic chain, with an average value $\hbar\omega \sim 0.43$ MeV, whereas for the $\pi g_{9/2}^{-1}$ bands the corresponding average value is $\hbar\omega \sim 0.36$ MeV. It is expected that the difference observed in the two crossing frequencies may be the result,

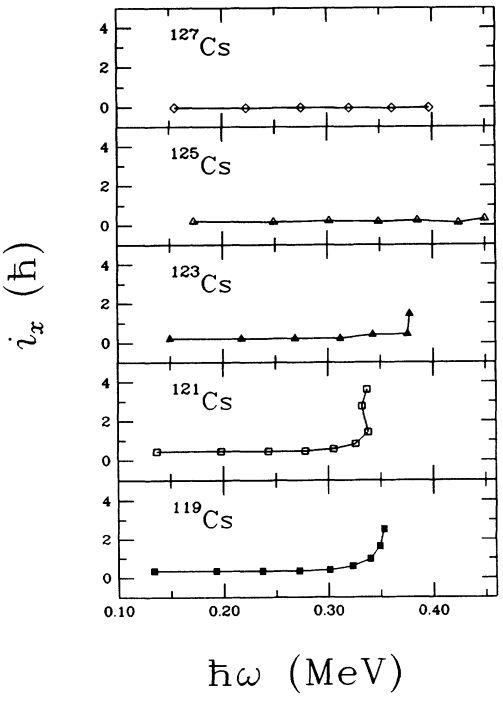

FIG. 5. Experimental alignments i_x of the $\pi g_{9/2}^{-1}$ bands in the odd-mass Cs isotopes from $N = 64$–72. A reference rotor has been extracted independently in each case, from a fit to the low-lying members of the $\pi g_{9/2}^{-1}$ bands. The experimental data are taken from the present work and Refs. [10,16–18].

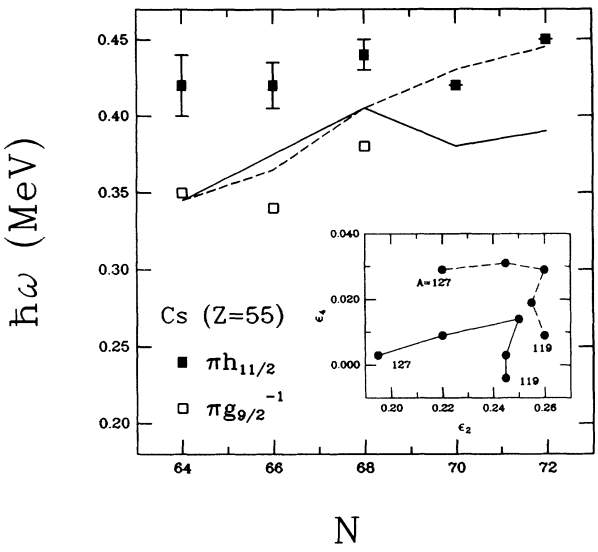

FIG. 6. Experimental $[\nu h_{11/2}]^2$ crossing frequencies for the $\pi h_{11/2}$ (solid squares) and $\pi g_{9/2}^{-1}$ (open squares) bands, for the odd-mass Cs isotopes. Also shown are the results of a CSM calculation for the $\pi h_{11/2}$ (solid line), and the $\pi g_{9/2}$ (dashed line) configurations, using deformation parameters ($\epsilon_{2,4}$) appropriate for the bandhead of the given configuration taken from PES results shown in the inset. The experimental data have been taken from the present work and Refs. [10,16–18].

in part, of different deformations in the two configurations. Consequently, potential energy surface (PES) calculations have been performed to determine the deformations of the two configurations.

The deformation parameters appropriate for both the $\pi h_{11/2}$ and $\pi g_{9/2}^{-1}$ bandheads have been extracted from axially symmetric PES calculations at zero rotational frequency, using the Nilsson-Strutinsky method with the newly fitted (κ,μ) parameters [9], and including a monopole pairing term [7]. The pairing gap parameter is taken as 80% [37] of that obtained from odd-even mass differences from neighboring even-even nuclei (except for ^{119}Cs, where it is extrapolated from the heavier isotopes), and is kept the same for both configurations, as an approximation. The extracted deformation parameters ($\epsilon_{2,4}$) are found to be consistent with those obtained from axially symmetric PES calculations using the Woods-Saxon potential [38], and TRS calculations [33] performed at a frequency just below the first crossing.

The crossing frequency results of the CSM calculations using the deformation parameters extracted from the PES calculations are displayed in Fig. 6 (the deformation parameters are shown inset). It is apparent that the differences in the deformations of the two configurations do not affect the crossing frequency to a large extent for $N \leq 68$ (the PES calculations show that the quadrupole deformations in the two configurations are similar for these isotopes). For $N > 68$, however, the calculations do show that the $\nu h_{11/2}$ crossing should occur at a lower frequency in the $\pi h_{11/2}$ band than in the $\pi g_{9/2}^{-1}$ band. This effect can be attributed to the substantially larger quadru-

pole deformation (ϵ_2) in the $\pi g_{9/2}^{-1}$ band with respect to that in the $\pi h_{11/2}$ band for the $N > 68$ isotopes. It should be noted that although the magnitude of the crossing frequency in the $\pi h_{11/2}$ band is consistently underestimated, the trend is rather well reproduced. The striking feature in the lighter isotopes ($N \leq 68$), however, is that the $[\nu h_{11/2}]^2$ pair alignment in the $\pi h_{11/2}$ band is delayed relative to that in the $\pi g_{9/2}^{-1}$ band; a feature that is not reproduced in the calculations.

A similar delayed crossing frequency has recently been observed in the light ^{117,119}I [4,5] nuclei. In the case of ^{117}I it has been noticed that a quadrupole deformation $\epsilon_2 \sim 0.29$ is necessary to reproduce the crossing frequency in the $\pi h_{11/2}$ band, whereas $\epsilon_2 \sim 0.25$ gives good agreement in the $\pi g_{9/2}^{-1}$ band. The PES calculations, however, suggest that the quadrupole deformation in the $\pi h_{11/2}$ bands of both the light Cs and I nuclei, is similar to that in the corresponding $\pi g_{9/2}^{-1}$ bands ($\epsilon_2 \sim 0.25$).

In contrast to the iodine nuclei, where a weak band interaction is observed in the $\pi h_{11/2}$ bands, the light cesium nuclei show a strong band interaction. This implies a significant mixing between the bands above and below the crossing (manifest as a gradual upbend of i_x as a function of $\hbar\omega$). However, while the magnitude of the interaction strength does affect the nature of the crossing, it is not expected to shift the crossing frequency.

As previously discussed, $B(M1)/B(E2)$ ratios indicate that the $\pi h_{11/2}$ band may have a degree of triaxiality both below ($\gamma \sim 10°$) and above ($\gamma \sim -15°$) the $\nu h_{11/2}$ crossing. However, while the CSM results do show that a small positive $\gamma(\sim 10°)$ would increase the $\nu h_{11/2}$ crossing frequency by 6–7 % for ^{123}Cs, conversely, a negative $\gamma(\sim -15°)$ would decrease the crossing frequency by $\sim 10\%$. As discussed in Ref. [39], the crossing frequency cannot be extracted from a CSM calculation performed at one fixed deformation. Alternatively, the crossing frequency may be estimated by taking the average of the values obtained at the two deformations. The results of this procedure lower the predicted crossing frequencies for all but the lightest Cs isotopes, where the value converges with that obtained at $\gamma = 0°$ [17].

IV. CONCLUSIONS

Several collective structures have been populated in the transitional ^{123}Cs nucleus following the ^{108}Pd(^{19}F,4n) fusion-evaporation reaction. Positive-parity structures based on the $g_{7/2}$ proton and the $g_{9/2}$ proton-hole orbitals have been confirmed and extended. The medium spin structure, however, is found to be dominated by configurations based on the unique-parity $\pi h_{11/2}$ orbital. Both signatures of the single-quasiparticle configuration are observed, thus allowing a precise determination of the signature splitting. The alignment of this band shows a gradual upbend as a function of rotational frequency, attributed to the effects of $[\nu h_{11/2}]^2$ pair alignment. The signature splitting decreases through the alignment, indicating that a degree of triaxiality may be introduced by the aligning neutrons. In addition, the neutron pair alignment is observed to occur at a relatively higher crossing frequency than that in the $\pi g_{9/2}^{-1}$ band. PES calculations using the Nilsson-Strutinsky method with monopole pairing cannot reproduce this difference with a configuration dependent deformation. This feature is not well understood at present. Finally, a well developed γ-vibrational band based on the $\pi h_{11/2}$ orbital is observed to feed both signature components of the corresponding rotational structure.

ACKNOWLEDGMENTS

We would like to thank Dr. R. Wyss for supplying us with the TRS mesh. This work was supported in part by the National Science Foundation. One of us (JYZ) would like to acknowledge the support of NSF Grant No. INT-9001476.

[1] I. Ragnarsson, A. Sobiczewski, R. K. Sheline, S. E. Larsson, and B. Nerlo-Pomorska, Nucl. Phys. **A233**, 329 (1974).

[2] Y. S. Chen, S. Frauendorf, and G. A. Leander, Phys. Rev. C **28**, 2437 (1983).

[3] G. Andersson, S. E. Larsson, G. Leander, P. Möller, S. G. Nilsson, I. Ragnarsson, S. Aberg, R. Bengtsson, J. Dudek, B. Nerlo-Pomorska, K. Pomorski, and Z. Szymański, Nucl. Phys. **A268**, 205 (1976).

[4] E. S. Paul, M. P. Waring, R. M. Clark, S. A. Forbes, D. B. Fossan, J. R. Hughes, D. R. LaFosse, Y. Liang, R. Ma, P. Vaska, and R. Wadsworth, submitted to Phys. Rev. C.

[5] Y. Liang, D. B. Fossan, J. R. Hughes, D. R. LaFosse, T. Lauritsen, R. Ma, and E. S. Paul, Phys. Rev. C **45**, 1041 (1992).

[6] J. C. Bacelar, R. Chapman, J. R. Leslie, J. N. Mo, E. Paul, A. Simcock, J. C. Wilmott, J. D. Garret, G. B. Hagemann, B. Herskind, A. Holm, and P. M. Walker, Nucl. Phys. **A442**, 547 (1985); R. A. Bark, G. D. Dracoulis, A. E. Stuchberry, A. P. Byrne, A. M. Baxter, F. Riess, and P. K. Weng, *ibid.* **501**, 157 (1989); M. A. Riley, J. Simpson, R. Aryaeinejad, J. R. Cresswell, P. D. Forsyth, D. Howe, P. J. Nolan, B. M. Nyakó, J. F. Sharpey-Schaffer, P. J. Twin, J. Bacelar, J. D. Garrett, G. B. Hagemann, B. Herskind, and A. Holm, Phys. Lett. **135B**, 275 (1984).

[7] N. Xu, J.-Y. Zhang, Y. Liang, R. Ma, E. S. Paul, and D. B. Fossan, Phys. Rev. C **42**, 1394 (1990).

[8] Y. Liang, R. Ma, E. S. Paul, N. Xu, D. B. Fossan, J.-Y. Zhang, and F. Dönau, Phys. Rev. Lett. **64**, 29 (1990).

[9] J.-Y. Zhang, N. Xu, D. B. Fossan, Y. Liang, R. Ma, and E. S. Paul, Phys. Rev. C **39**, 714 (1989).

[10] Y. Liang, Ph.D. thesis, Stony Brook, New York (1991).

[11] M. P. Waring, D. B. Fossan, J. R. Hughes, D. R. LaFosse, Y. Liang, and P. Vaska (unpublished).

[12] Y. Liang, D. B. Fossan, J. R. Hughes, D. R. LaFosse, R. Ma, T. Lauritsen, E. S. Paul, P. Vaska, M. P. Waring, N. Xu, and R. Wyss, Phys. Rev. C **44**, R578 (1991).

[13] S. Juutinen, S. Törmänen, B. Cederwall, A. Johnson, R. Julin, S. Mitarai, J. Mukai, P. Ahonen, B. Fant, F. Lidén,

J. Nyberg, and I. Ragnarsson, Z. Phys. A **338**, 365 (1991).
[14] J. Simpson, H. Timmers, M. A. Riley, T. Bengtsson, M. A. Bentley, F. Hanna, S. M. Mullins, J. F. Sharpey-Shafer, and R. Wyss, Phys. Lett. B **262**, 388 (1991).
[15] R. Wyss, F. Lidén, J. Nyberg, A. Johnson, D. J. G. Love, A. H. Nelson, D. W. Banes, J. Simpson, A. Kirwan, and R. Bengtsson, Z. Phys. A **330**, 123 (1988); R. Wyss, A. Johnson, D. J. G. Love, M. J. Godfrey, and S. M. Mullins, *ibid.* **332**, 241 (1989).
[16] P. Vaska, D. B. Fossan, J. R. Hughes, D. R. LaFosse, Y. Liang, and M. P. Waring (unpublished).
[17] J. R. Hughes, D. B. Fossan, D. R. LaFosse, Y. Liang, P. Vaska, and M. P. Waring, Phys. Rev. C **44**, 2390 (1991).
[18] Y. Liang, R. Ma, E. S. Paul, N. Xu, and D. B. Fossan, Phys. Rev. C **42**, 890 (1990).
[19] G. Beyer, R. Arlt, E. Hermann, A. Jasinski, O. Knotek, G. Musiol, H. G. Ortlepp, H. V. Siebert, and J. Tyroff, Nucl. Phys. **A260**, 269 (1976).
[20] P. Arlt, A. Jasinski, W. Neubert, and H.-G. Ortlepp, Acta Phys. Pol. B **6**, 433 (1975).
[21] U. Garg, T. P. Sjoreen, and D. B. Fossan, Phys. Rev. C **19**, 217 (1979).
[22] J. Hattula, S. Juutinen, M. Jääskeläinen, T. Lönroth, A. Pakkanen, M. Piiparinen, and G. Sletten, J. Phys. G **13**, 57 (1987).
[23] J. R. Hughes, D. B. Fossan, D. R. LaFosse, Y. Liang, P. Vaska, and M. P. Waring, Bull. Am. Phys. Soc. Vol. **36**, 1360 (1991).
[24] L. Hildingsson, C. W. Beausang, D. B. Fossan, W. F. Piel, Jr., A. P. Byrne, and G. D. Dracoulis, Nucl. Instrm. Methods Sect. A **252**, 91 (1986).
[25] T. Yamazaki, Nucl. Data A **3**, 1 (1967).
[26] R. D. Gill, *Gamma ray Angular Correlations* (Academic, New York, 1975), p. 180.
[27] R. Bengtsson and S. Frauendorf, Nucl. Phys. **A327**, 139 (1979).
[28] S. M. Harris, Phys. Rev. **138**, B509 (1965).
[29] R. E. Shroy, A. K. Gaigalas, G. Schartz, and D. B. Fossan, Phys. Rev. C **19**, 1324 (1979); W. F. Piel, Jr., P. Chowdhury, U. Garg, M. A. Quadar, P. M. Swertka, S. Vadja, and D. B. Fossan, Phys. Rev. C **31**, 456 (1985); R. E. Shroy, D. M. Gordon, M. Gai, D. B. Fossan, and A. K. Gaigalas, *ibid.* **26**, 1089 (1982).
[30] L. Hildingsson, C. W. Beausang, D. B. Fossan, R. Ma, E. S. Paul, W. F. Piel, Jr., and N. Xu, Phys. Rev. C **39**, 471 (1989).
[31] F. Dönau and S. Frauendorf, in *Proceedings of the Conference on High Angular Momentum Properties of Nuclei, Oak Ridge, 1982,* edited by N. R. Johnson (Harwood Academic, New York 1983), p. 143; F. Dönau, Nucl. Phys. **A471**, 469 (1987).
[32] A. L. Larabee, L. H. Courtney, S. Frauendorf, L. L. Riedinger, J. C. Wadington, M. P. Fewell, N. R. Johnson, I. Y. Lee, and F. K. McGowan, Phys. Rev. C **29**, 1934 (1984).
[33] R. Wyss, J. Nyberg, A. Johnsson, R. Bengtsson, and W. Nazarewicz, Phys. Lett. B **215**, 211 (1988).
[34] J. R. Hughes, D. B. Fossan, D. R. LaFosse, Y. Liang, P. Vaska, and M. P. Waring (unpublished).
[35] L. Hildingsson, W. Klamra, Th. Lindblad, F. Lidén, Y. Liang, R. Ma, E. S. Paul, N. Xu, D. B. Fossan, and J. Gascon, Z. Phys. A **340**, 29 (1991).
[36] J. P. Martin, V. Barci, H. El-Samman, A. Gizon, J. Gizon, W. Klamra, and B. M. Nyakó, Nucl. Phys. **A489**, 169 (1988).
[37] R. Bengtsson and J.-Y. Zhang, Phys. Lett. **135B**, 358 (1984).
[38] W. Nazarewicz, J. Dudek, R. Bengtsson, T. Bengtsson, and I. Ragnarsson, Nucl. Phys. **A435**, 397 (1985); W. Nazarewicz (private communication).
[39] W. C. Ma, A. V. Ramayya, J. H. Hamilton, S. J. Robinson, J. D. Cole, E. F. Zganjar, E. H. Spejewski, R. Bengtsson, W. Nazaewicz, and J.-Y. Zhang, Phys. Lett. **167B**, 277 (1986).